



香港城市大學
City University of Hong Kong

專業 創新 胸懷全球
Professional · Creative
For The World

CityU Scholars

Erp57 facilitates ZIKV-induced DNA damage via NS2B/NS3 complex formation

Wang, Yiran; Song, Dan; Li, Yichen; Qin, Leiying; Wan, Qianya; Hu, Huan; Wu, Mandi; Feng, Yaxiu; Schang, Luis; Weiss, Robert; He, Ming-Liang

Published in:

Emerging Microbes & Infections

Published: 01/12/2024

Document Version:

Final Published version, also known as Publisher's PDF, Publisher's Final version or Version of Record

License:

CC BY-NC

Publication record in CityU Scholars:

[Go to record](#)

Published version (DOI):

[10.1080/22221751.2024.2417864](https://doi.org/10.1080/22221751.2024.2417864)

Publication details:

Wang, Y., Song, D., Li, Y., Qin, L., Wan, Q., Hu, H., Wu, M., Feng, Y., Schang, L., Weiss, R., & He, M.-L. (2024). Erp57 facilitates ZIKV-induced DNA damage via NS2B/NS3 complex formation. *Emerging Microbes & Infections*, 13(1), Article 2417864. <https://doi.org/10.1080/22221751.2024.2417864>

Citing this paper

Please note that where the full-text provided on CityU Scholars is the Post-print version (also known as Accepted Author Manuscript, Peer-reviewed or Author Final version), it may differ from the Final Published version. When citing, ensure that you check and use the publisher's definitive version for pagination and other details.

General rights

Copyright for the publications made accessible via the CityU Scholars portal is retained by the author(s) and/or other copyright owners and it is a condition of accessing these publications that users recognise and abide by the legal requirements associated with these rights. Users may not further distribute the material or use it for any profit-making activity or commercial gain.

Publisher permission

Permission for previously published items are in accordance with publisher's copyright policies sourced from the SHERPA RoMEO database. Links to full text versions (either Published or Post-print) are only available if corresponding publishers allow open access.

Take down policy

Contact lbscholars@cityu.edu.hk if you believe that this document breaches copyright and provide us with details. We will remove access to the work immediately and investigate your claim.



Erp57 facilitates ZIKV-induced DNA damage via NS2B/NS3 complex formation

Yiran Wang, Dan Song, Yichen Li, Leiying Qin, Qianya Wan, Huan Hu, Mandi Wu, Yaxiu Feng, Luis Schang, Robert Weiss & Ming-Liang He

To cite this article: Yiran Wang, Dan Song, Yichen Li, Leiying Qin, Qianya Wan, Huan Hu, Mandi Wu, Yaxiu Feng, Luis Schang, Robert Weiss & Ming-Liang He (2024) Erp57 facilitates ZIKV-induced DNA damage via NS2B/NS3 complex formation, *Emerging Microbes & Infections*, 13:1, 2417864, DOI: [10.1080/22221751.2024.2417864](https://doi.org/10.1080/22221751.2024.2417864)

To link to this article: <https://doi.org/10.1080/22221751.2024.2417864>



© 2024 The Author(s). Published by Informa UK Limited, trading as Taylor & Francis Group, on behalf of Shanghai Shangyixun Cultural Communication Co., Ltd



View supplementary material [↗](#)



Published online: 28 Oct 2024.



Submit your article to this journal [↗](#)



Article views: 489



View related articles [↗](#)



View Crossmark data [↗](#)

Erp57 facilitates ZIKV-induced DNA damage via NS2B/NS3 complex formation

Yiran Wang^{a#}, Dan Song^{a#}, Yichen Li^a, Leiying Qin^a, Qianya Wan^a, Huan Hu^a, Mandi Wu^a, Yaxiu Feng^a, Luis Schang^b, Robert Weiss^c and Ming-Liang He^{a,d}

^aDepartment of Biomedical Sciences, City University of Hong Kong, Hong Kong SAR, People's Republic of China; ^bDepartment of Microbiology and Immunology, College of Veterinary Medicine, Cornell University, Ithaca, NY, USA; ^cDepartment of Biomedical Sciences, College of Veterinary Medicine, Cornell University, Ithaca, NY, USA; ^dCityU Shenzhen Research Institute, Shenzhen, People's Republic of China

ABSTRACT

It is believed that DNA double-strand breaks induced by Zika virus (ZIKV) infection in pregnant women is a main reason of brain damage (e.g. microcephaly, severe brain malformation, and neuropathy) in newborn babies [1,2], but its underlying mechanism is poorly understood. In this study, we report that the depletion of Erp57, a member of the protein disulphide isomerase (PDI) family, leads to the limited production of ZIKV in nerve cells. Erp57 knockout not only suppresses viral induced reactive oxygen species (ROS) mediated host DNA damage, but also decreases apoptosis. Strikingly, DNA damage depends on Erp57-bridged complex formation of viral protein NS2B/NS3. LOC14, an Erp57 inhibitor, restricts ZIKV infection and virus-induced DNA damage. Our work reveals an important role of Erp57 in both ZIKV propagation and virus-induced DNA damage, suggesting a potential target against ZIKV infection.

ARTICLE HISTORY Received 20 June 2024; Revised 13 September 2024; Accepted 13 October 2024

KEYWORDS Erp57; ZIKA virus; DNA damage; ZIKV NS2B/NS3 complex; antiviral; ROS; apoptosis




Introduction

Mosquito-borne flaviviruses, such as dengue virus (DENV), West Nile virus (WNV) and Zika virus (ZIKV), have garnered significant global attention due to their heightened transmissive rate and the escalating incidence of congenital brain abnormalities [1,3,4]. Particularly noteworthy is the firmly established causal relationship between ZIKV infection during pregnancy and fetal microcephaly [5,6]. ZIKV possesses a single-stranded positive RNA genome which is translated into a large polyprotein. Subsequently, this polyprotein undergoes proteolytic processing by host and viral proteases, leading to the production of three structural proteins and seven nonstructural proteins [7,8]. Recent research have increasingly focused on elucidating the functional roles of ZIKV nonstructural proteins, as they play indispensable roles in viral life cycle [9]. Notably, ZIKV nonstructural protein 1 (NS1) exhibits the ability to modulate the host antibody response and may contribute to virus-induced oxidative stress [10]. In addition, NS4A and NS4B are believed to manipulate host cell innate immune responses and autophagy [11,12]. Furthermore, the combination of NS2B and NS3 has been implicated in the cleavage and


subsequent inactivation of the mitochondrial-bound enzymes [13–15].

Given that brain damage is a prominent consequence of ZIKV infections, investigating its underlying mechanism holds great promise for the development of antiviral drugs. The accumulation of DNA damage emerges as a significant factor contributing to brain malfunctions [16–18]. Research demonstrated that DNA damage markers serve as indicators for individuals experiencing brain damage following mild traumatic brain injury (mTBI) [19]. Most viruses inevitably engage in host cell DNA process, whether through modulating gene expression and cellular DNA replication or due to viral genome integration. This probably triggers DNA damage response (DDR), which is an evolutionary mechanism aimed at preserving genetic integrity [20]. ATM (Ataxia telangiectasia mutated) and ATR (ataxia telangiectasia and Rad3-related protein), members of phosphoinositide 3 (PI-3) kinase families, are activated in response to DNA double-strand breaks (DSB) or single strand breaks (SSB) respectively. They subsequently regulate cell cycle progression and apoptosis [21].

Existing evidence suggests that ZIKV infection leads to DNA double-strand breaks through activating

CONTACT Ming-Liang He  minglihe@cityu.edu.hk; Robert Weiss  rsw26@cornell.edu  Department of Biomedical Sciences, College of Veterinary Medicine, Cornell University, Ithaca, NY, 14853, People's Republic of China

[#]Those authors contributed equally.

 Supplemental data for this article can be accessed online at <https://doi.org/10.1080/22221751.2024.2417864>.

© 2024 The Author(s). Published by Informa UK Limited, trading as Taylor & Francis Group, on behalf of Shanghai Shangyixun Cultural Communication Co., Ltd This is an Open Access article distributed under the terms of the Creative Commons Attribution-NonCommercial License (<http://creativecommons.org/licenses/by-nc/4.0/>), which permits unrestricted non-commercial use, distribution, and reproduction in any medium, provided the original work is properly cited. The terms on which this article has been published allow the posting of the Accepted Manuscript in a repository by the author(s) or with their consent.

ATM/Chk2 pathway [2]. It is also reported that ZIKV can impede host cell replication by arresting cells in S phase [2]. However, the specific mechanisms involving host protein in this process remain elusive, and the responsible viral protein is still veiled. ERp57 is a member of protein disulphide isomerases (PDIs), known for its multifunctional oxidoreductase and chaperone functions involved in catalyzing disulphide bond formation, isomerization, and reduction within the ER [22]. Considering the essential roles of PDIs in oxidative protein folding and maintaining ER homeostasis, they have emerged as potential contributors to a spectrum of diseases, including virus infection. The overexpression of PDI has been implicated in facilitating viral membrane fusion, indicating a potential mechanism by which viruses exploit the PDI family to gain entry into host cells [23]. Moreover, recent findings by Marco et al. have conducted redox proteomics analysis of HPV positive tissues, revealing a positive correlation between ERp57 expression level and tissue redox status [24]. This observation suggests a potential association between ERp57 and viral-induced oxidative DNA and protein damage. Additionally, studies have demonstrated a diminished replication of influenza A and B virus with knockdown of ERp57 [25]. However, the specific relationship between ERp57 and ZIKV has never been described.

In this study, we investigated the pivotal role of ERp57 (PDIA3), an ER chaperone protein, in ZIKV-induced DNA damage and viral activities. We show that ERp57 is critical for ZIKV-induced endoplasmic reticulum stress (ER stress) and reactive oxygen species (ROS) production. Mechanistically, ERp57 serves as a facilitator for the formation of ZIKV NS2B and NS3 complex, leading to increased DNA damage, apoptosis, and viral infections. These findings provide insight to the mechanism of ERp57 in supporting ZIKV infections, suggesting a potential target for developing antiviral strategies against ZIKV infections.

Results

ERp57 depletion suppresses ZIKV production in vitro

Stress proteins, known as chaperon proteins, are actively synthesized and play a crucial role in responding to various cellular stresses and virus infections. Previously, our group illustrated that heat shock proteins (HSPs), including Hsp90 β , Hsc70, Hsp27, and ERp57, are important for enterovirus A71 (EV-A71) infection [26–29]. However, apart from GRP78 and Hsp70, limited information is available regarding the functions of other HSPs in Zika virus (ZIKV) infection. RD cells are extensively used to study the

infections by ZIKV and other viruses [30,31]. In this study, we discovered that both intracellular and extracellular ZIKV RNA level and envelope protein level decreased in the Hsp90 β knockout RD cells (Figure S1(A–D)). Similarly, silencing heat shock cognate protein 70 (Hsc70) also restricted ZIKV RNA levels and cytopathic effects (CPE) (Figure S1(E–H)).

Intriguingly, we observed an increased ERp57 level in a time-dependent manner with ZIKV infections (Figure S2(B)). To further explore the function of ERp57 on ZIKV infections, we constructed two ERp57 knockout RD cells (Figure S2(A and B)). Strikingly, sharply decreased intracellular ZIKV RNA levels were found in the two ERp57 knockout RD cell lines after 24 or 48 h infections. The second knockout cell line exhibited over 90% reduction in RNA levels at 48 h post-infection (Figure 1(A)). However, no noticeable changes were observed during the virus absorption and entry process within the initial 5-hour infection (Figure S2(C and D)). A previous study indicated that the ubiquitination of ZIKV envelope protein enhances viral entry by interacting with the receptor TIM1 [32]. In our study, we detected that ERp57 expression did not affect the RNA level of TIM1 (Figure S2(E)). This highlights the impact of ERp57 on other stages of the viral life cycle. Additionally, less obvious cytopathic effects (CPE) were also detected in the ERp57 knockout cells, shown by fewer rounding and detached cells (Figure 1(B)). Consistently, the plaque assay demonstrated a significant reduction in viral titres with ERp57 knockout (Figure 1(C) and S2(F)).

Moreover, we applied OM (Oblongifolin M), an inhibitor for PDI family proteins [27], to RD cells. In consistent with knockout cell results, less obvious CPE was discovered with OM treatment (Figure S2(G)). Since ZIKV can cause neurological disorders, the effect of ERp57 on ZIKV was further tested in human glioblastoma cells (U87) and neuroblastoma cells (SH-SY5Y) cell lines, which are widely used in studies of the Zika virus and neuroscience [33–35]. Similarly, a decreased intracellular RNA level was discovered in the ERp57 silencing U87 cells, and the extracellular RNA decreased over 60% with ERp57 knockdown (Figure 1(D) and S2(H)). Correspondingly, the viral titre in wild type cells was over 50 folds of the ERp57 silencing U87 cells (Figure 1(E)). ERp57 silencing also protected glioblastoma cells from severe CPE (Figure S2I). On the other hand, ZIKV envelope protein level significantly decreased in different ERp57 silencing cell lines, including RD, A549, U87, and SH-SY5Y (Figure 1(F–H) and S2(J)). Correspondingly, the expression of ZIKV envelope protein level increased in a dose-dependent manner with ERp57 overexpressed (Figure 1(I)). These results indicated that ERp57 plays an important role in ZIKV infections, which is cell type independent.

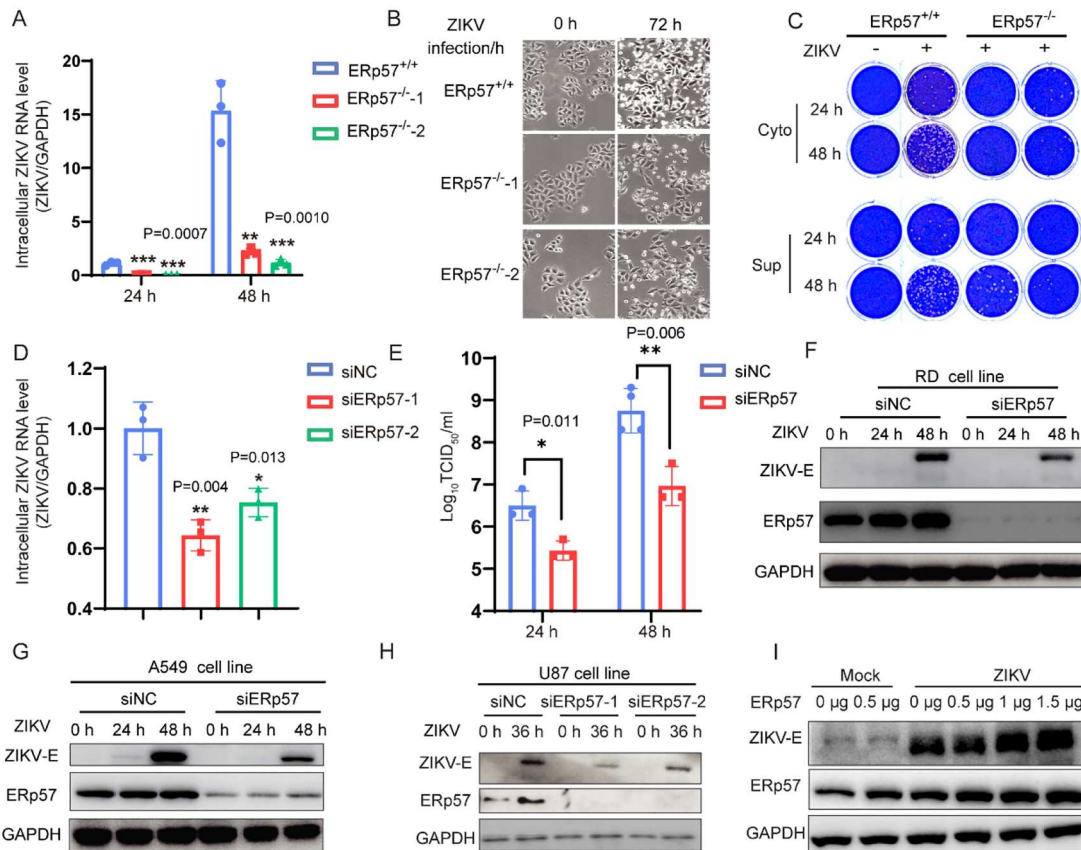


Figure 1. ERp57 depletion suppresses ZIKV production *in vitro*. (A) Wild type RD and ERp57-KO cells were infected with ZIKV (MOI = 1). Intracellular RNA samples were collected at the indicated time post infection, later used for quantitative RT-PCR. (B) Representative CPE images of wild type or ERp57-KO RD cells at 72 h after ZIKV (MOI = 1) or mock infection. CPE of ZIKV is indicated by rounding and detachment of cells. (C) Wild type RD or ERp57-KO cells were infected with ZIKV (MOI = 1). Infectious viral particles in culture supernatants and cell lysates were measured by plaque assay. (D) and (E) U87 cells were transfected with scramble siRNA or siERp57 for 24 h. Cells were infected by ZIKV (MOI = 1) for 24 h. Intracellular RNA samples were collected and used for quantitative RT-PCR (D). Viral titre was determined by TCID₅₀ after the indicated viral infection time (E). (F)–(H) RD or A549 or U87 cells were transfected with scramble siRNA or siERp57 for 24 h. Cells were then infected by ZIKV (MOI = 1) for the indicated time and protein samples were analysed by western blot. (I) Wild type RD cells were transfected with ERp57 plasmid for overexpression. Cells were infected by ZIKV (MOI = 1) with 24 h and protein samples were harvested at the indicated time. Viral titres and qRT-PCR data are means ± SEM from three independent experiments. * $P \leq 0.05$, ** $P \leq 0.01$, *** $P \leq 0.001$, **** $P \leq 0.0001$ (unpaired *t*-test).

ERp57 depletion reduces ZIKV-induced ER stress and ROS production

ZIKV is known for inducing ER stress due to the overwhelming burden placed on ER folding machinery [36]. In our study, we discovered that ZIKV infection triggered a robust upregulation level of GRP94, an ER stress protein, and C/EBP homologous protein (CHOP), a key marker of ER stress-induced apoptosis. Remarkably, the depletion of ERp57 effectively restricted the upregulation of these ER stress markers (Figure 2(A,B,D), and S2(K)). The unfolded protein response (UPR) is a cellular mechanism activated in response to ER stress for restoring the homeostasis in ER and ensuring normal protein folding. Strikingly, we observed that ZIKV infection induces upregulation of UPR-associated markers phosphorylated EIF2 α and IRE1 α (Figure 2(C,D)). Notably, the increased level of these markers was significantly attenuated upon

ERp57 depletion, highlighting the regulatory role of this ER chaperone protein.

Considering the intricate interplay between ER stress and ROS, we sought to investigate the potential involvement of ERp57 in ZIKV-induced ROS generation, given its pivotal role in oxidative folding processes. Our investigations revealed a discernible augmentation in ROS levels after ZIKV infections. Notably, the wild-type cells exhibited significantly higher ROS levels in comparison to the ERp57 knock-out RD cells (Figure 2(E)). Additionally, a significant decrease in ROS fluorescence intensity was observed in the ERp57-silenced A549 cells after ZIKV infection, as shown by confocal imaging, microplate reader analysis, and flow cytometry (Figures 2(F–I)). These compelling findings underscore the indispensable role of ERp57 in orchestrating ZIKV-triggered ER stress and ROS induction, highlighting its

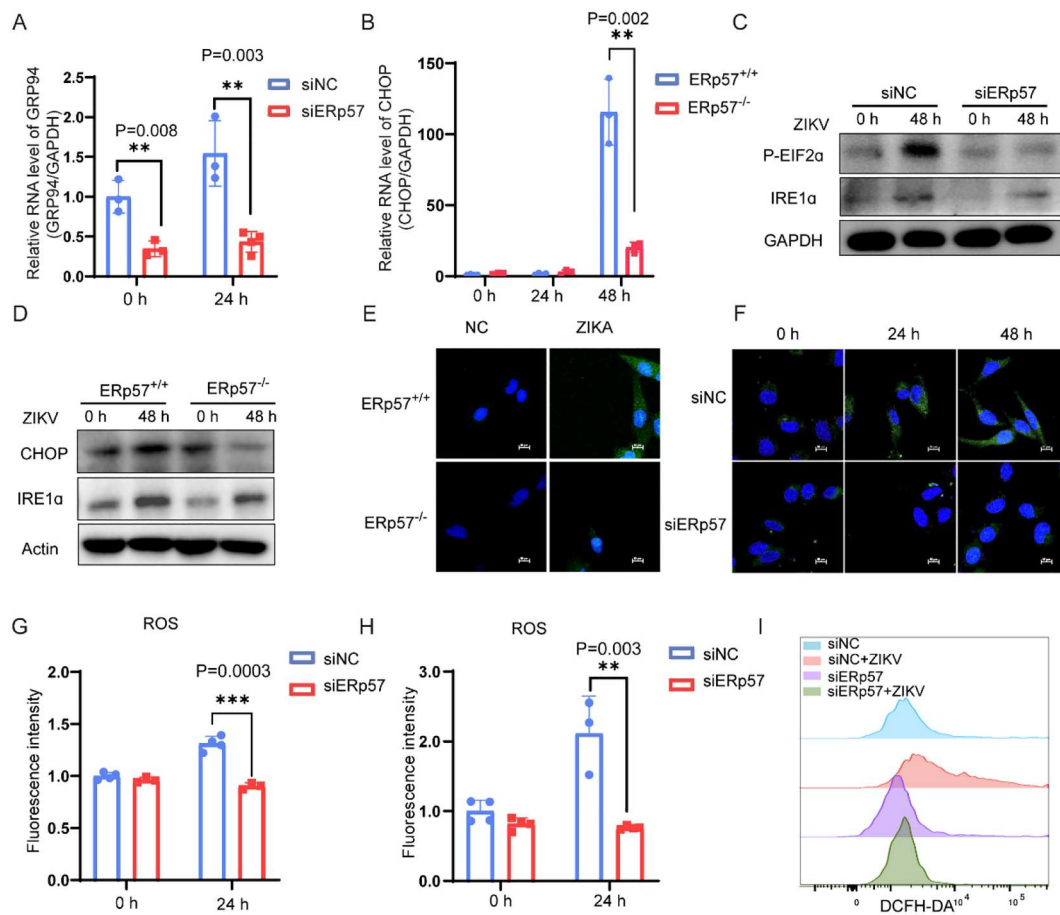


Figure 2. ERp57 depletion inhibits ZIKV-induced ER stress and ROS production. (A) U87 cells were transfected with scramble siRNA or siERp57 for 24 h. Intracellular RNA samples were collected after 24 h infection, later used for quantitative RT-PCR. (B) Wild type RD and ERp57-KO cells were infected with ZIKV (MOI = 1). Intracellular RNA samples were collected at indicated time point, later used for quantitative RT-PCR. (C) RD cells were transfected with scramble siRNA or siERp57 for 24 h. Protein samples were harvested after 48 h ZIKV infection (MOI = 1). (D) Both wild-type and knockout RD cells were infected with ZIKV (MOI = 1) for 48 h and the protein expression were analysed by western blot. (E) Immunofluorescence images showing ROS in WT and KO RD cells. Cells were infected with or without Zika virus (MOI = 1) for 24 h. Cells were stained with ROS (green) and DAPI (blue) and visualized under confocal microscope. (F–I) A549 cells were transfected with either scramble siRNA or siERp57 for 24 h, followed by ZIKV infection for the indicated time. ROS production was stained and measured by confocal image (green) (F), microplate reader (G), and flow cytometry (H and I). Results were expressed as mean \pm standard deviation (error bars) of at least three repeats. * $P \leq 0.05$, ** $P \leq 0.01$, *** $P \leq 0.001$, **** $P \leq 0.0001$ (unpaired *t*-test).

multifaceted involvement in the cellular response to ZIKV infection.

ERp57 depletion decreases ZIKV-induced host cell DNA damage

ROS is a well-known inducer of DNA damage and ZIKV is found to cause DNA damage [37,38]. We employed 8-oxoguanine, a widely recognized marker for oxidative DNA damage [39,40], to investigate the potential contribution of ERp57 on ROS induced DNA lesion. In the wild-type RD cells with ZIKV infection, we observed a progressive increase in the number of green foci, thereby suggesting heightened DNA lesions resulting from oxidative stress after ZIKV infection, whereas 8-oxo-foci was barely visible even after 48 h of ZIKV challenge in the ERp57-depleted cells (Figure 3(B) and S3(A)).

To further confirm our finding, we performed the neutral comet assay to assess the DNA double strand breaks (DSBs) generated by ZIKV infection [41]. By evaluating the length of comet-like tails, we uncovered a physical increase in DNA DSBs upon ZIKV infection. Notably, the presence of ERp57 is necessary for the generation of host cell DNA damage, as evidenced by shorter and smaller comet tail length in the knockout cells (Figure 3(A)). These findings provided strong evidence that ZIKV infection could induce oxidative DNA damage, wherein the involvement of ERp57 is critical.

To further validate our results, we conducted immunofluorescence and immunoblotting assays to examine γ -H2AX activation, a key marker of DNA damage response initiation. In wild-type cells, ZIKV infection led to a significant increase in γ -H2AX level, particularly after 48 h. However, ERp57

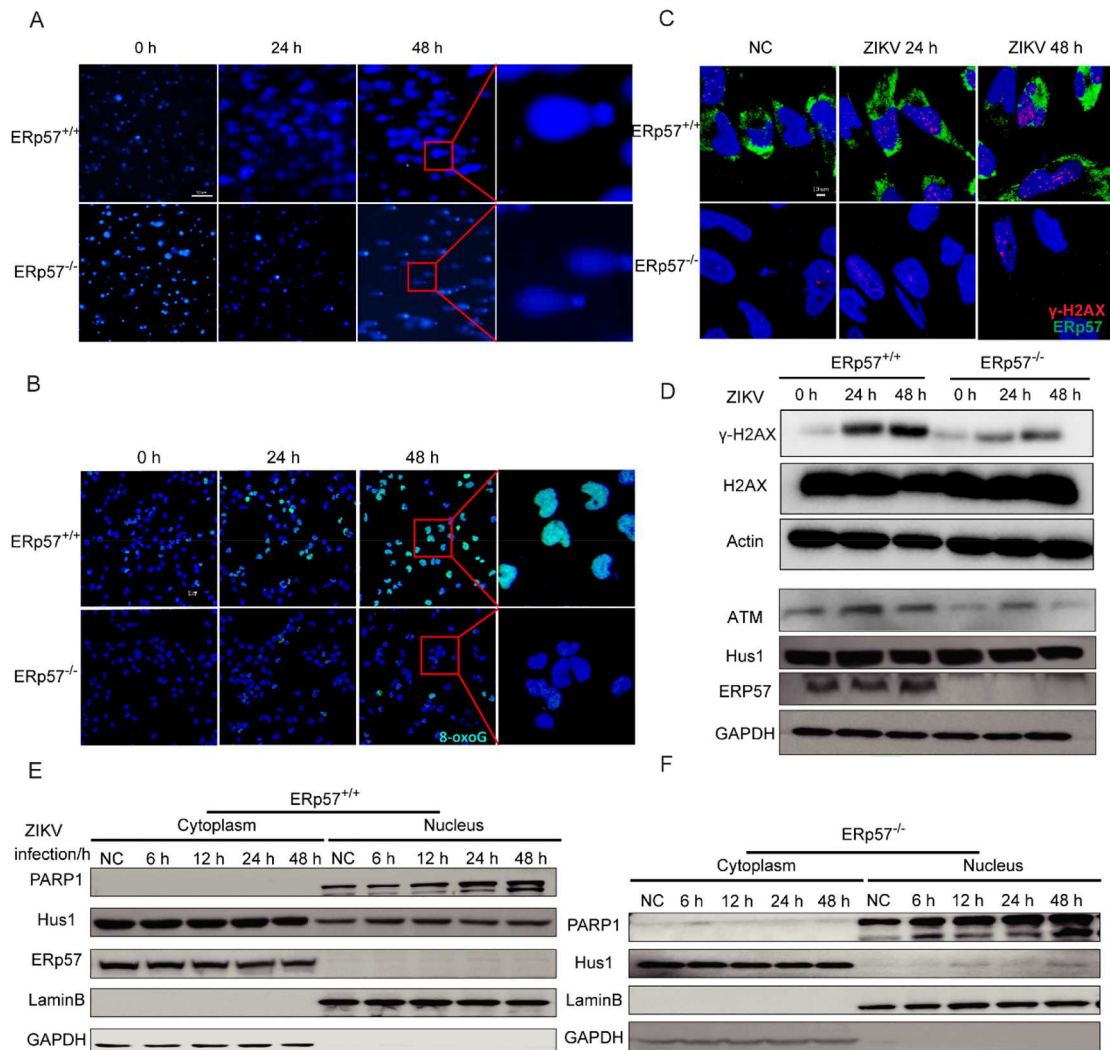


Figure 3. ERp57 depletion decreases ZIKV-induced host cell DNA damage. (A) Representative comet assay images of ZIKV-induced DNA fragmentation. Cells were infected with Zika virus (MOI = 1) 24 h or 48 h before being harvested. Each round dot represents the original cell nuclear area, while the comet shaped tails to the left indicate fragmented DNA. The bigger the DNA tail area or the longer the DNA tail length, the more significant the damage. (B) Immunofluorescence images showing accumulated 8-oxoguanine within WT and KO RD cells. Cells were infected with Zika virus (MOI = 1) 24 h or 48 h before being harvested. Cells were fixed and stained with anti 8-oxoG (green) fluorescence antibody and DAPI (blue) and visualized under confocal microscope. (C) Immunofluorescence images showing foci of gamma H2AX within nucleus of ZIKA infected RD cells. WT and ERp57-KO RD cells were infected with ZIKA virus (MOI = 1) for the indicated time. The cells were fixed and stained with anti-gamma H2AX (red) and ERp57 (green) fluorescence antibody afterwards. (D) Wild type or knockout RD cells were infected with ZIKA virus (MOI = 1). Cell lysate was collected at the indicated time point, and protein expressions were analysed over a time course. (E) and (F) Wild type or knockout RD cells were infected by ZIKV at MOI = 10 for the indicated time. Nuclear and cytosol protein were extracted and separated by Beyotime Kit. The protein expressions were analysed by western blot.

knockout cells exhibited consistently low levels of γ -H2AX foci (Figure 3(C–D) and S3(B–C)). Similar results were observed in the U87 cell lines and SH-SY5Y (Figure S3(D–E)). We also discovered that H_2O_2 treatment (ROS induction) triggered more DNA damage with the help of ERp57 (Figure S3(F)). Furthermore, we assessed the expression and activation level of other DDR related factors. When sensing a DSB, ATM kinase can phosphorylate and activate γ -H2AX at Ser-139 (γ -H2AX) [42,43]. An elevation of ATM level was also detected after virus infection in the wild type cells, while ERp57 knockout cells exhibited lower expression levels (Figure 3(D)).

In addition, Rad1, Rad9, and Hus1 are recruited and formed a 9-1-1 complex when sensing DDR. Under normal conditions, Hus1 predominantly remains in the cytoplasm, while its nucleus localization requires Rad9's nuclear localization signal (NLS) upon DNA damage sensing [44]. We observed that the expression level of Hus1 and Rad9 remained consistent regardless of the presence of ERp57 (Figure 3(D) and S3(G–H)). However, in the wild type cells, a significant proportion of Hus1 localized in the nucleus, while in the knockout cells, the majority remained in the cytosol, even following ZIKV infection (Figure 3(E,F)). Furthermore, a co-immunoprecipitation assay showed that the binding of Hus1 and

Rad9 only existed in the wild-type RD cells with ZIKV infection, indicating reduced DNA damage in the knockout cells (Figure S3(I)).

Moreover, we investigated the level of PARP1 (poly (ADP-ribose) polymerase 1), a key marker in DNA repair process. We detected a great increase of PARP1 level in the nucleus after ZIKV infection (Figure 3(E,F)). However, the expression of PARP1 was lower in the ERp57 knockout cells, suggesting diminished DNA damage and repair (Figure S3(J)). Collectively, these results strongly support the requirement of ERp57 for ZIKV-induced DNA lesion and subsequent DDR activation.

ERp57 depletion inhibits ZIKV-induced apoptotic cell death

Apoptosis is a common consequence of DNA damage for protecting normal cellular activities from damaged cells. To elucidate the mechanism by which ERp57 depletion suppressed ZIKV infection induced cell death, we conducted the flow cytometry experiment. Both the early (Annexin positive/PI negative) and late apoptotic cells (Annexin positive/PI positive) dramatically increased after ZIKV infection as compared to the mock group and the apoptotic cells could be observed as early as 24 h post ZIKV infection. More importantly, the percentage of cells in both early and late apoptotic stages showed a significant drop in the ERp57 knockout groups compared to wild type cells (Figure 4(A,B)).

p53 plays a central role in DNA damage response and acts as a coordinator in DNA repair by halting cell cycle and inducing apoptosis. We first observed an increased level of p53 with ZIKV infection, which was consistent with others finding that ZIKV can elicit p53 activation and apoptosis (Figure 4(C) and S4(A–B)) [45]. Interestingly, the RNA level of p53 decreased about 38% in the ERp57 knockdown U87 cells compared to the wild type cells after 36 h ZIKV infection (Figure 4(C)). Similar results were found in p53 protein level (Figure S4(A and B)). Moreover, the expression level of p21, a p53-inducible protein, remained low in the ERp57 knockout RD cells (Figure S4(B)), which illustrated the importance of ERp57 in DNA damage-induced apoptosis after ZIKV infection.

On the other hand, we also analysed several signal transducers of the apoptosis pathway to confirm the results. A marked increase could be observed in the activation level of pro-apoptosis factor, Bax, after ZIKV infection in the wild type cells, while their expression maintained low in either ERp57 knockout RD cells or ERp57 silencing U87 cells (Figure 4(D–E and G) and S4(C)). Remarkably, the RNA level of BAX decreased over 66% in the knockout cells compared to wild type cells after 48 h infections (Figure 4(E)). On the other hand, the expression and

phosphorylation level of anti-apoptosis factors, including Bcl-xL, Bcl-2, and GSK3B was higher in the ERp57 depleted cells (Figure 4(F–G) and S4(D)). More importantly, the cleaved form of caspase 3 and 8, the key regulators of apoptosis, were reduced in the ERp57 knockout cells (Figure 4(H)). These findings demonstrated that ERp57 played a key role in ZIKV-induced apoptotic cell death.

ERp57 is critical for ZIKA nonstructural protein expression and function

Numerous studies have elucidated the significance of ZIKV nonstructural proteins in viral life cycle and their impact on viral activities. We hypothesized that ERp57 may influence the expression levels of these nonstructural proteins, thereby modulating the subsequent DNA damage response. Consistent to other's findings [46], ZIKV NS5, the viral RNA dependent RNA polymerase (RdRp), was predominately located within host cell nuclei (Figure 5(A)). Interestingly, the existence of ERp57 does not affect either the localization or the expression of NS5 (Figure 5(A,B)). However, we detected an interesting pattern that the expression of NS1, NS2B, and NS3 decreased markedly in the knockout RD cells (Figure 5(C)). A similar result was found in the ERp57 silencing nerve cells (Figure S5(A and B)).

Given the previous data highlighting the significance of NS1 in ER remodelling [47], our focus shifted towards investigating the impact of ERp57 affects NS1 expression and its associated DNA damage. Consistent with the western blot result, a significant decrease of NS1 was detected in the ERp57 knockout cells, shown by immunofluorescence (Figure 5(D)). To further validate if NS1 is necessary for ZIKV-induced DNA damage, we transfected NS1-Flag expression plasmid into cells during ZIKV infection and performed immunoblotting to analyse several signal transducers of the DDR and apoptosis pathway (Figure 5(E)). Consistent with the previous data, we detected a reduced expression level of DNA damage marker (γ -H2AX) and pro-apoptosis factor (Bax), accompanied by an elevated level of the anti-apoptosis factor (Bcl-2) in the ERp57-depleted cells after ZIKV infection compared to the wild type cells. However, NS1 significantly restored the level of γ -H2AX and Bax while decreasing the expression of Bcl-2 in the knockout cells, proving that NS1 protein helped ZIKV-induced DNA damage response and apoptosis.

However, the presence of ERp57 did not influence NS1 induced DDR and apoptosis when cells were not infected with ZIKV simultaneously. In the wild type cells, the expression of γ -H2AX level increased, while Bcl-2 level reduced after NS1 transfection. However, those protein levels were similar in both wild type and the ERp57 knockout cells with NS1

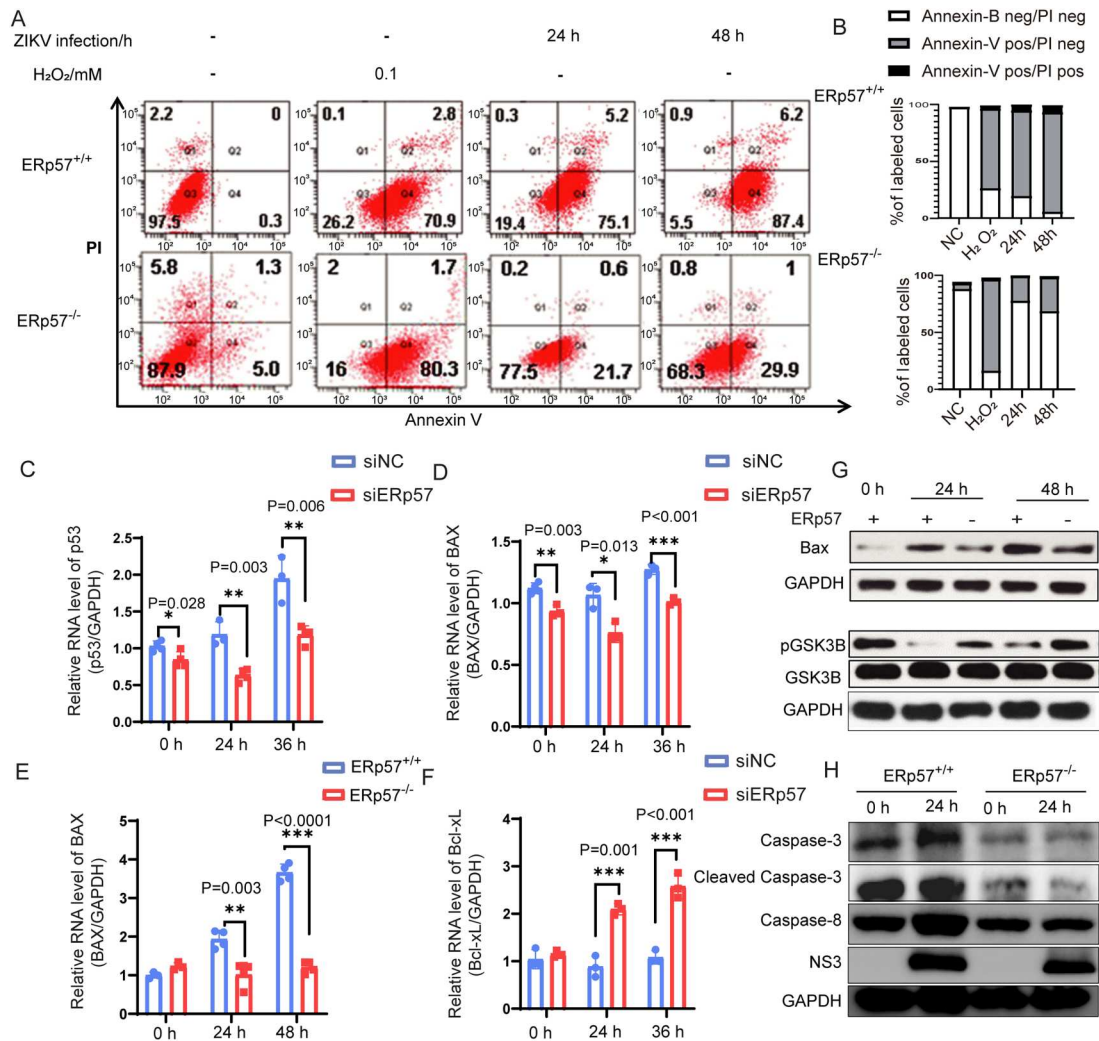


Figure 4. ERp57 depletion inhibits ZIKV-induced apoptotic cell death. (A) and (B) Flow cytometry analysis of ZIKV-induced early-stage apoptosis. WT or ERp57-KO RD cells were treated with PBS or ZIKV (MOI = 1) dilution 24 h or 48 h before sample collection. Cells treated with hydrogen peroxide (H₂O₂, 0.1 mM) 1 h before collection were used as positive controls. The statistical results of the proportion of healthy (double negative), early apoptotic (Annexin V positive), late apoptotic (double positive) and necroptotic (double positive) cell populations are shown as percentage (B). (C) and (D) and (F) U87 cells were transfected with scramble siRNA or siERp57 for 24 h. Cells were then infected by ZIKV (MOI = 1) for the indicated time. Intracellular RNA samples were then collected and used for quantitative RT-PCR. (E) Both wild type RD cells and knockout cells were infected by ZIKV (MOI = 1) for the indicated time. Intracellular RNA samples were then collected and used for quantitative RT-PCR. (G) and (H) Representative images show the protein expression level of apoptosis related regulators in ZIKV-infected WT or ERp57-KO RD cells. RD cells were infected with ZIKA (MOI = 1), and protein expression analysed over indicated time course. * $P \leq 0.05$, ** $P \leq 0.01$, *** $P \leq 0.001$, **** $P \leq 0.0001$ (unpaired *t*-test).

expression (Figure 5(F)). Together, these results suggested that ZIKV NS1 protein is important for viral induced host cell DDR and apoptosis, but it does not depend on ERp57.

ERp57 helps NS2B and NS3 binding to promote DDR

Since ERp57 expression did not influence the NS1 induced DDR and apoptosis, we assumed that other ZIKV proteins were involved in this process. The viral proteases NS2B and NS3 complex formation is important for viral transcription and many other viral activities [48,49]. First, we discovered that the γ -H2AX expression was higher in wild type RD cells

with NS2B or NS3 expression alone, compared to the knockout RD cells (Figure 6(A) and S6(C)). Surprisingly, the increased level of γ -H2AX became more obvious with NS2B and NS3 coexistence (Figure 6(A) and S6(A–B)), while its level was still low in the KO cells (Figure 6(A)). Similarly, a decreased γ -H2AX level was detected in ERp57-silenced SH-SY5Y cells with NS2B and NS3 transfection (Figure S6(D)). Additionally, we used immunofluorescence to further illustrate this finding. In the ERp57 knockout cells, the intensity of γ -H2AX produced by NS2B or NS3 decreased markedly (Figure 6(B,C)). More importantly, the existence of both NS2B and NS3 expanded the DNA damage on wild type cells, while the influence on the knockout cells was still minimum (Figure 6

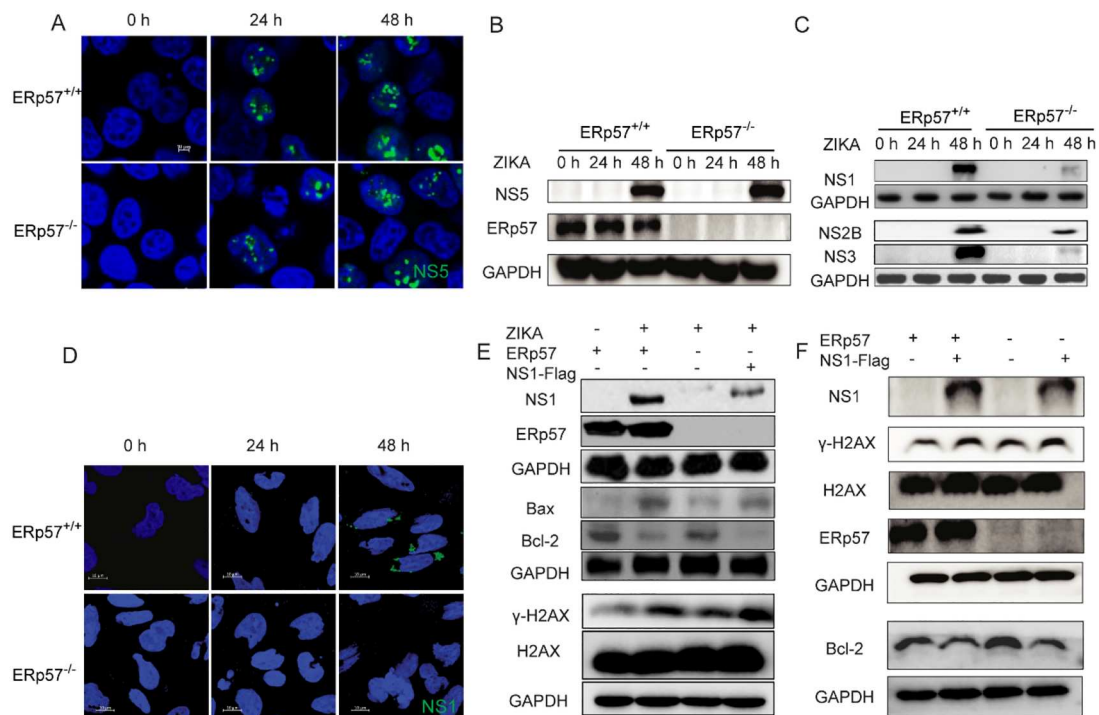


Figure 5. ERp57 is critical for ZIKA nonstructural protein expression and function. (A) Representative immunofluorescent staining images show the localization of ZIKV NS5 (green). WT RD cells were seeded in 24-well plates with pre-coated cover glasses, then infected with ZIKA virus (MOI = 1) for the indicated time. Cells were fixed and stained with anti-NS5 (green) fluorescence antibody and DAPI (blue) and visualized under confocal microscope. (B) and (C) Both wild type RD cells and knockout cells were infected by ZIKV (MOI = 1) at the indicated time and protein level was analysed by western blot. (D) Both WT and KO RD cells were infected with ZIKV (MOI = 1) for the indicated time. Cells were fixed and stained with anti-NS1 (green) fluorescence antibody and DAPI (blue) and visualized under confocal microscope. (E) Both wild type RD cells and ERp57-KO cell line were transfected with NS1-flag plasmid or vector, then infected with ZIKV (MOI = 1) for 48 h. Protein samples were blotted to investigate the expression level of NS1 and other DDR related factors. (F) Western blot images of WT and ERp57-KO cells transfected with NS1-Flag plasmid or vector for 24 h.

(D)). Further, an elevated ROS level was detected in wild type cells after co-transfecting NS2B and NS3 (Figure S6(E)). Therefore, NS2B and NS3 complex can cause ROS and severe DNA damage to cells and ERp57 is important during this process.

The next question raised to us: how does ERp57 get involved in NS2B and NS3 complex and induce DNA damage. We first confirmed the binding between NS2B and NS3 in the wild-type RD cells (Figure 6(E) and S6(F)). Surprisingly, we detected an interaction between ERp57 and NS2B, but not with NS3, by immunofluorescence and Co-immunoprecipitation assay (Figure 6(F) and S6(F–G)). However, the interaction between ERp57 and NS3 appears with NS2B existence, and their binding is likely to be located on ER (Figure S6(H)). We further wondered if the binding of ERp57 and NS2B could impact the formation of NS2B and NS3 complex. Interestingly, we observed a decreased binding between these two proteases in the ERp57 knockout cells (Figure 6(G–I)). Similar results were confirmed by confocal images (Figure 6(E)). These indicated that the interaction between ERp57 and NS2B promoted the binding of NS2B and NS3 in the wild type cells. However, the generation of NS2B and

NS3 complex was interfered in the knockout cells, which caused less severe DNA damage to cells. Therefore, ERp57 is the key factor to bridge NS2B and NS3 complex formation for the induction of DNA damage.

ERp57 inhibitor decreases ZIKV infection and virus-induced DNA damage

A previously reported ERp57 reversible modulator, LOC14, can bind to the active site of ERp57 and decrease its reductase activities [50]. LOC14 was found to decrease ER stress and influenza A level [51,52]. We therefore examined the effect of LOC14 on ZIKV infections. The CCK-8 assay showed that LOC14 only affects cell growth at high concentration (Figure S7(A)). Moreover, we discovered that LOC14 significantly decreases ZIKV RNA level (Figure 7 (A)). Both ZIKV envelope and NS3 protein levels were also inhibited by LOC14 in a dose-dependent manner (Figure 7(B)). Notably, the ZIKV-induced CPE and viral titre were attenuated after LOC14 treatment (Figure 7(C) and S7(B–C)). Additionally, confocal microscopy results showed a decreased ZIKV envelope level upon LOC14 treatment (Figure S7(D)).

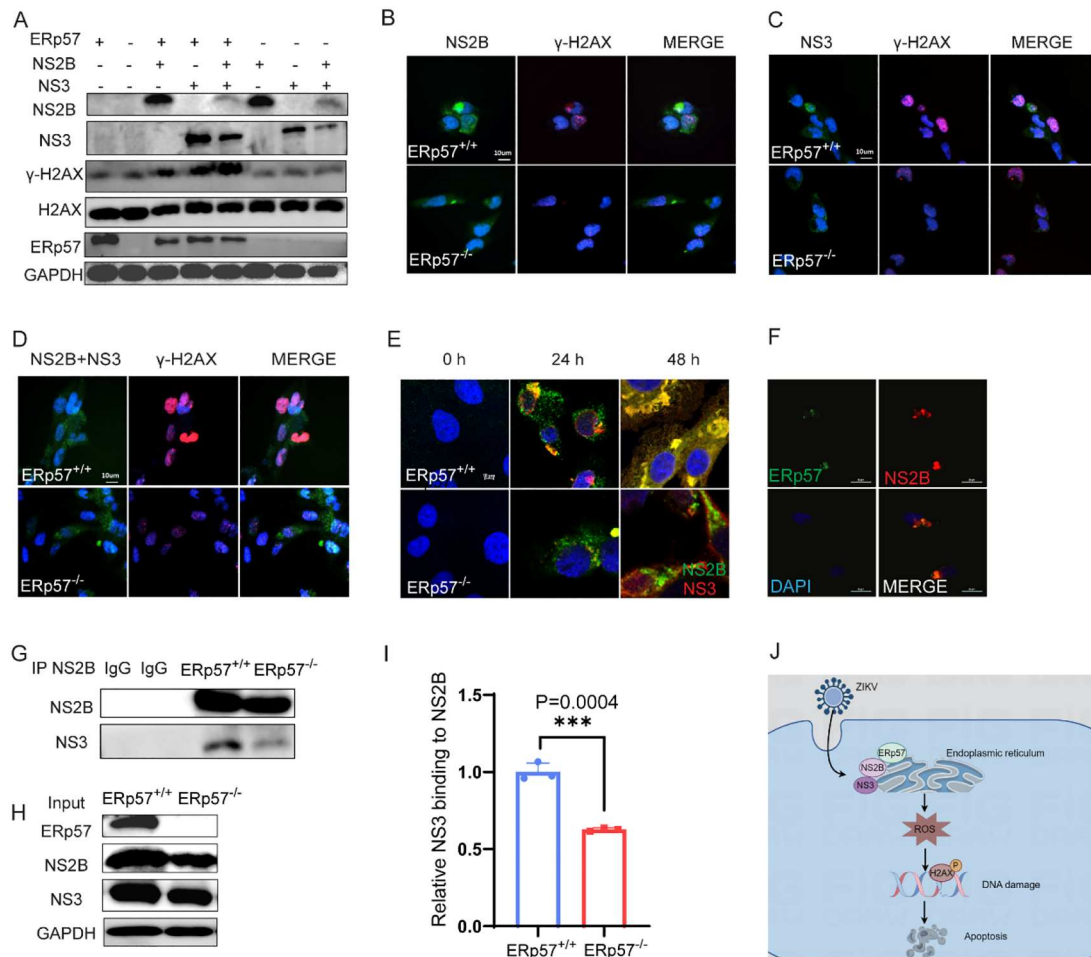


Figure 6. ERp57 helps NS2B and NS3 binding to promote DDR. (A) Both wild type RD cells and ERp57 knockout cells were transfected by NS2B, NS3 plasmids for 24 h and protein level was analysed by western blot. (B)–(D) Both wild type RD cells and ERp57 knockout cells were infected by NS2B (B), NS3 (C) lentivirus or their combinations (D). The cells were fixed and stained with anti-γ-H2AX (red) and NS2B (green) or NS3 (green). (E) RD cells were seeded in 24-well plates with pre-coated cover glasses, then infected with ZIKA virus (MOI = 1) for 24 or 48 h after cultured for 24 h. Cells were fixed and stained with anti-NS2B (green) fluorescence antibody and NS3 (red) and visualized under confocal microscope, yellow indicates the co-localization of the two proteins. (F) RD cells were infected with ZIKV for 24 h at MOI = 1. The cells were fixed and stained with ERp57 (green) and NS2B (red). (G)–(I) Both wild type RD cells and knockout cells were infected with ZIKV for 48 h at MOI = 1. Whole cell lysates (H) and immunoprecipitated proteins incubated with anti-NS2B antibody (G) were analysed by immunoblotting. GAPDH was used as a loading control for the inputs while IgG was used as the negative control for the co-immunoprecipitation experiments. The densitometric analysis of NS2B and NS3 levels in Figure 6(G), along with the total NS3 level in Figure 6(H), was quantified. The NS2B-bound NS3 was first analysed by NS3 level relative to pulled NS2B from Figure 6(G). Additionally, the ratio of NS2B-bound NS3 to total NS3 from the input sample was further analysed (I). (J) The schematic picture shows the interaction between ERp57 and ZIKV proteins.

To further illustrate the importance of ERp57 in ZIKV-induced DNA damage, we treated cells with different concentrations of LOC14 along with ZIKV infections. We observed a dose dependent reduction in γ-H2AX with LOC14 treatment (Figure 7(D)). A similar result was confirmed by immunofluorescence image (Figure 7(E)). Both phosphorylated EIF2α and Caspase 3 level decreased with LOC14 treatment, indicating restricted ER stress and apoptosis (Figure S7 (E)). Since ERp57 is critical for ZIKV NS2B and NS3 proteins to induce DNA damage, we used LOC14 to further confirm this mechanism. Interestingly, LOC14 inhibited γ-H2AX levels caused by NS2B and NS3 transfection, shown by both western blot and confocal image (Figure 7(E,F)). Our findings demonstrate that the ERp57 inhibitor, LOC14, can effectively

inhibit ZIKV replication and virus-induced DNA damage, suggesting its potential as a therapeutic candidate against ZIKV infections.

Discussion

Stress proteins are known to play critical roles in maintaining homeostasis in host cells. Recently, their involvement in viral infections has gained particular attention. Previous research found the interaction between GRP78, an ER-resident chaperone protein, and ZIKV envelope protein, highlighting the role of ER proteins in ZIKV replication [53]. Here, we identified another ER chaperone protein, ERp57, shares a close relationship with ZIKV infections. Previous work demonstrated the involvement of ERp57 on

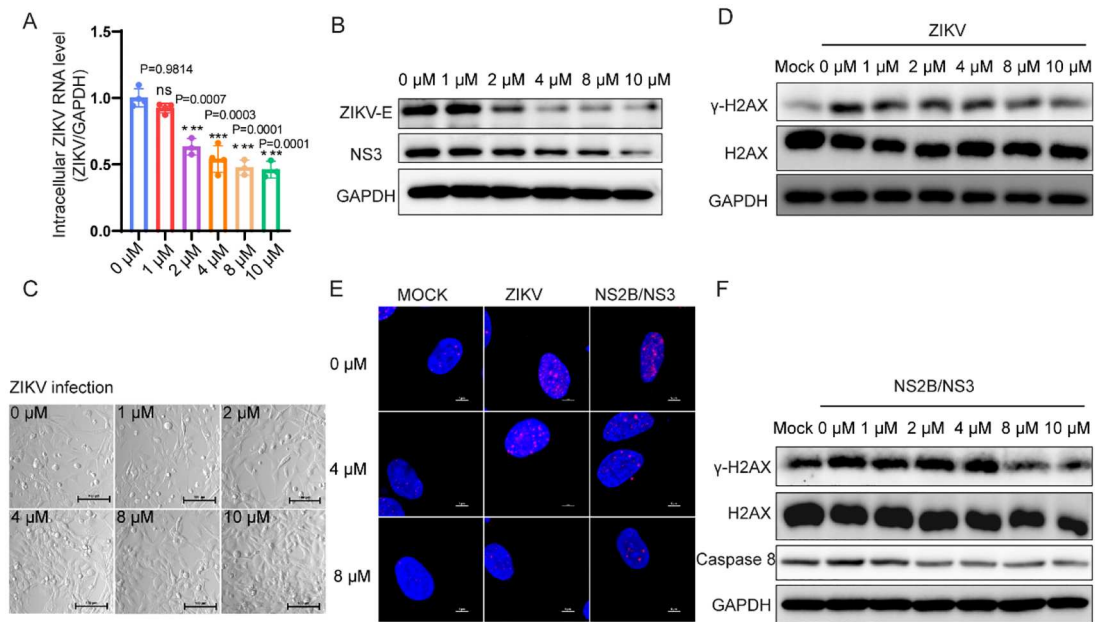


Figure 7. LOC14 decreases ZIKV-induced DNA damage. (A–C) RD cells were treated with the indicated concentrations of LOC14 for 2 h, then infected with ZIKV at an MOI of 1 for 24 h. DMSO was treated in 0 μM group. Intracellular viral RNA level was tested by RT-qPCR (A) and viral protein level was determined by western blot (B). Representative CPE images of RD cells were indicated by rounding and detachment of cells (C). Cells without ZIKV infections are in Figure S7(B). (D) RD cells were treated with different concentrations of LOC14 for 2 h, then infected with ZIKV (MOI = 1) for 24 h. Protein level was further analysed by western blot. (E) RD cells were treated with different concentrations of LOC14 for 2 h, and RD cells were infected with ZIKA virus (MOI = 1) or NS2B and NS3 transfection for 24 h. The cells were fixed and stained with anti-gamma H2AX (red) and Hoechst (blue) afterwards. (F) RD cells were pretreated with LOC14 for 2 h and transfected with NS2B and NS3 for 24 h. Protein levels were analysed by western blot. * $P \leq 0.05$, ** $P \leq 0.01$, *** $P \leq 0.001$, **** $P \leq 0.0001$ (unpaired *t*-test).

neurodegenerative diseases [54], suggesting its potential relevance in the context of ZIKV, which is associated with neurological complications. Indeed, we observed a significant decrease in viral load after silencing ERp57 expression in human glioblastoma cells (U87) and neuroblastoma cells (SH-SY5Y). This finding uncovers a distinctive association between ERp57 and viral infections, providing further insights into the intricate interplay between ER proteins and pathogenesis. When viruses invade cells, they initiate the production of various viral proteins and cause an accumulation of unfolded or misfolded host proteins. This disrupts ER homeostasis, resulting in ER stress, which is linked to oxidative stress due to the dysregulated disulphide bond formation [55]. Several studies have highlighted the role of ER stress and the disruption of redox balance in the establishment of Zika virus infections [38,56]. ERp57, a thiol-disulphide oxidoreductase, is responsible for catalyzing the formation, isomerization, and reduction of disulphide bonds within ER. This underscores the significant role of ERp57 in ZIKV-induced ER stress and ROS generation. Our study demonstrated that ERp57 facilitated the formation of the NS2B and NS3 complex. Additionally, we observed reduced levels of the ER stress marker IRE1 α and decreased ROS levels in ERp57-silenced cells. The accumulation of ROS may further influence viral pathogenesis and cellular responses.

Viral infections are found to participate in host cell DNA regulation and probably cause DNA damage. For example, DNA viruses possess genomes capable of directly activating DDR, triggered by viral DNA entry or replication. RNA viruses such as retrovirus which undergo reverse transcription and rely on a DNA intermediate for replication, can also activate DDR. Notably, a retroviral protein, HIV-1 Tat protein, involved in viral transcription, has been reported to induce increased ROS production and DNA damage [57]. Although ZIKV does not undergo reverse transcription, previous research also found it has been linked to DNA damage [2]. Besides this, we revealed a decreased level in H2AX phosphorylation in the ERp57 silenced nerve cells, which indicates that ERp57 acts as a key regulator in ZIKV-induced DNA damage. Given the accumulation of DNA damage is recognized as a significant factor contributing to brain dysfunction, this suggests that ERp57 can potentially mitigate brain damage caused by ZIKV infection.

Apoptosis, a programmed cell death process, is often triggered when excessive DNA damage is produced that cannot be effectively repaired. The activation of the tumour suppressor protein p53 is usually preceded for apoptosis and prevents the propagation of cells with DNA damage, which further induces the expression of other pro-apoptosis factors,

such as BAX. In our study, we discovered a promoted level of p53 and BAX in both RD and U87 cell lines upon ZIKV infections, indicating as a cell type independent activity. However, the expression of those factors decreased significantly in the ERp57 depleted cells. Together, these results suggested that ERp57 is necessary for the induction of DNA damage and subsequent apoptotic response caused by ZIKV infection.

Emerging evidence revealed that ZIKV nonstructural proteins target various host proteins, facilitating viral replication and survival. NS5 has the potential to impact host DNA damage by directly binding to host DNA and regulating gene transcription [58]. Although we confirmed the presence of NS5 in the nucleus, its expression does not change with or without ERp57. However, we found that ERp57 can affect ZIKV NS1 protein expression, but the ability of NS1 to manipulate the host cell's DDR and apoptosis does not require ERp57. Other research demonstrated that NS1 interacted with GRP78 and the NS1 expression was inhibited by GRP78 inhibitor treatment [59]. Subsequently, we identified that NS2B and NS3 probably serve as the key mediators. The DNA damage markers upregulated significantly with NS2B and NS3, while their levels dropped in the ERp57-depleted cells. Previous studies found the formation of NS2B and NS3 complex is important for viral replication, and various compounds have been designed to target this complex for antiviral purposes [60,61]. Flavivirus NS2B functions as a cofactor and the binding with NS3 is necessary for the proteolytic processing of polyproteins [62]. Interestingly, previous research has demonstrated that NS3 alone can induce apoptosis independently of NS2B. In our research, we revealed that while γ -H2AX level slightly decreased in the ERp57 knockout cells with NS2B or NS3 alone, the difference became significantly more pronounced when NS2B and NS3 were present simultaneously. This indicated that the complex formation of NS2B and NS3 acts as a key regulator for ERp57 dependent DNA damage caused by ZIKV.

Then we thought to investigate the involvement of ERp57 in the induction of DNA damage by NS2B and NS3. ZIKV NS2B is a transmembrane protein, with its N and C termini tightly associated with ER membrane [63], indicating a potential interaction between NS2B and ERp57. To test this hypothesis, immunofluorescence assays and Co-IP experiments were performed, providing evidence for the physical association between NS2B and ERp57. Moreover, this interaction was found to facilitate the formation of the NS2B/NS3 complex. Previous study has demonstrated that ZIKV NS3 itself localizes within mitochondrial, while NS2B serves as a recruiter, directing NS3 to the ER. Notably, NS2B mutations that lacks the help of NS3 protease activity inhibit ZIKV replication [64]. This probably explains that the disrupted binding between NS2B

and NS3, resulting from the absence of ERp57, leads to attenuated ZIKV infections. Additionally, NS2B and NS3 complex, the serine protease, is essential for polypeptide cleavage and the production of other viral proteins [13]. This offers a rationale for the decreased NS1 expression in the ERp57 knockout cells. Consequently, our work uncovers that the interaction between NS2B and ERp57 emerges as a critical determinant in NS2B/NS3 induced DNA damage.

In conclusion, our study provides novel insights into the role of ERp57 in ZIKV replication and propagation. We have discovered that ZIKV induces DNA damage and apoptosis, and this effect is attenuated in the ERp57 depleted cells. Additionally, we have identified that NS2B/NS3 complex as a key regulator of ZIKV-induced DNA damage, with ERp57 facilitating the interaction between these proteins. This observation explains the reduced DNA damage in the ERp57 knockout cells during ZIKV infection (Figure 6(J)). More importantly, the ERp57 inhibitor, LOC14, significantly decreases ZIKV infection and ZIKV-induced DNA damage. Our findings unveil a previously uncharacterized mechanism by which ZIKV nonstructural proteins contribute to DNA damage. The findings from this study are not only useful to design additional studies to unravel the underlying mechanism of ZIKV pathogenesis and tropism on neural tissue, but also helpful to develop strategies against ZIKV infections.

Materials and methods

Virus, cells, and reagents

Human rhabdomyosarcoma cell line (RD), U87 (human glioblastoma cell line), HEK293 cells were cultured using Dulbecco's modified Eagle's medium (DMEM, Gibco) with 10% fetal bovine serum (FBS, Gibco) and 10 U/ml penicillin-streptomycin (PS, Gibco) in a humidified incubation chamber with 5% CO₂ at 37°C. Cell cultured adapted MR766 ZIKV strain (VR-1838) was purchased from ATCC on 90% confluent monolayer cells in DMEM with 2% FBS. Virus titres were determined by plaque assays in RD cells.

Oblongifolin M (OM) is an inhibitor for PDI family proteins [27]. The inhibitor powder was dissolved in DMSO, and then diluted to desired concentration with blank DMEM medium. OM solution was added to RD cells directly after ZIKV infection and left in the culture medium until cells were collected for data analysis.

Knockout by CRISPR-Cas9/sgRNA

Two sgRNAs targeting ERp57 were designed and inserted in the lentiCRISPRv2 vectors. Lentiviral vectors were generated in HEK 293 T cells. RD cells were infected and selected with puromycin. Cell colonies

were obtained from single cells, and the effects of knockout were detected by western blot assays.

Plaque assay

Vero cells were seeded in a 12-well plate for 24 h. Cells were washed with PBS once and infected with virus samples for 1 h. The culture supernatant was aspirated and replaced with DMEM containing 1% low-melting agarose and 2% FBS. Viral plaques were stained with crystal violet solution and counted 4 days post infection.

TCID₅₀

RD cells were seeded into 96-well plates for 24 h before infection, then cells were infected by 100 µl per well of serial 10-fold diluted supernatant in quintuplicate. The 50% tissue culture-infected dose (TCID₅₀) was calculated by the Reed-Muench method after 96 h of infection.

RNA isolation, reverse transcription, and qRT-PCR

Total RNA from cells or viruses was extracted with TRIzol[®] (Thermo Fischer Scientific). Viral RNA copies were measured by qRT-PCR PrimeScript RT reagent Kit (Takara), as specified by manufacturers. SYBR[®] Premix Ex Taq[™] (Takara) was used to analyse mRNA levels on a StepOnePlus Real-Time PCR system (Applied Biosystems). The program is shown in following: 95°C for 30s followed by 40 cycles of 95°C for 5 s and 60°C for 30 s. Target gene's RNA transcriptional level was normalized to glyceraldehyde-3-phosphate dehydrogenase (GAPDH) in the same sample and results were calculated using $2^{-\Delta\Delta C_t}$ method. The primers used in this study were (Table 1):

Flow cytometry assay

Apoptosis

Treated cells were collected with trypsin and transferred to clean 1.5 ml microtubes. The collected cells were stained with a Propidium Iodine (PI) and Annexin V staining solution according to the manufacturer's instructions. Cells were selected depending on FSC and SSC and the gating of cell population was determined by healthy wild type RD cells. 10,000 cells per sample were analysed by BD FACSCanto machine (BD Biosciences). Cells were distinguished as follows: healthy cells (Annexin V⁻/PI⁻), early apoptotic (Annexin V⁺/PI⁻), late apoptotic (Annexin V⁺/PI⁺), and necroptotic (Annexin V⁺/PI⁺). Data were analysed by FlowJo software program.

Reactive oxygen species (ROS) detection assay

Treated cells were collected in 1.5 ml microtubes by trypsin. The assay was done by using ROS assay kit (Solarbio CA1410). Cells were stained with ROS fluorescent probe DCFH for 20 min with occasionally

shaking and were then washed by blank medium without FBS for three times. Stained samples were analysed using a BD FACSCanto machine (BD Biosciences) and data were analysed using FlowJo software.

Comet assay

The extent of DNA damage was evaluated by the comet assay, which was performed under alkaline conditions. A freshly prepared suspension of treated cells in 1% low melting point agarose dissolved in phosphate buffered saline was cast onto microscope slides precoated with 0.5% normal melting agarose. The cells were then lysed for 1 h at 4°C in a buffer consisting of 2.5 M NaCl, 100 mM EDTA, 1% Triton X-100, 10 mM Tris, pH 10. After the lysis, DNA was left to unwind for 40 min in electrophoretic solution consisting of 300 mM NaOH, 1 mM EDTA, pH > 13. Electrophoresis was conducted for 30 min at electric field strength 0.73 V/cm (30 mA). The slides were then neutralized with 0.4 M Tris, pH 7.5, and stained with DAPIs [31].

The slides were examined at fluorescence microscope (Nikon, Tokyo, Japan) equipped with a UV filter block consist of an excitation filter (359 nm) and barrier filter (461 nm) and connected to a personal computer-based image analysis system. 5–10 images were randomly taken from each experimental group.

Lentivirus package

Lentiviral vectors were prepared as described previously [65]. Briefly, HEK293 T cells were seeded in 10-cm cell culture dishes 24 h before transfection. Plasmids were transfected along with psPAX2 and pMD2.G lentivirus packaging system plasmids into HEK293 T cells. Plasmids containing genomes encoding ZIKV nonstructural proteins were purchased from Addgene, including NS1 (#79633), NS2B (#79637), NS3 (#79635), NS4a (#79636), NS5 (#79639). The supernatant of cells was collected and centrifuged after 48 h transfection and stocked in -80°C. Both wild type RD cells and ERp57 knockout cells were infected by lentiviruses for 48 h and then were selected in fresh medium containing puromycin.

Immunoblotting

WT and ERp57^{-/-} RD cells were either directly infected with ZIKV or transfected with the plasmids listed in the main text and, where indicated, infected with ZIKV afterwards. Cells were treated with lysis buffer after indicated time (50 mM tris-HCl (pH 7.5), 150 mM NaCl, 5 mM EDTA, 1% NP-40, 1 mM phenylmethylsulfonyl fluoride (PMSF), and 1× protease inhibitor (Roche), 1× Phostop (Roche) if needed). The cell extracts were immunoblotted with the indicated antibodies to measure the level of the

Table 1. The primers of the indicated genes [13].

	sense (5'-3')	antisense (5'-3')
GAPDH	GTCTCCTCTGACTTCAACAGCG	ACCACCTGTGCTGTAGCCAA
ZIKV	TGCCCAACACAAGGTGAAGC	ACTGACAGCATTATCCGGTACTC
p53	GAAATTTGCGTGTGGAGATTTG	GTTCCGTCCCAGTAGATTACCA
BAX	TCCCCCGAGAGGCTCTTT	CGGCCCCAGTTGAAGTTG
Bcl-xL	GGGTAACCTGGGGTCGCATTGTG	AAAGTATCCCAGCCGCCGTTCTC

expressed proteins. Anti- β -actin, anti-GAPDH, anti-ERp57 and other antibodies for apoptosis factors were purchase from Santa Cruz, anti-H2AX, anti-ATM and anti-p-ATM antibodies were purchased from Cell Signaling Technology, rabbit anti-ZIKV NS1 and other nonstructural protein antibodies were purchased from GeneTex, anti-Flag tag antibodies (Sigma-Aldrich) were also used for detection at the appropriate dilutions.

Immunoprecipitation and coimmunoprecipitation

WT and *ERp57*^{-/-} RD cells were infected by ZIKV at MOI = 1. Thirty hours after transfection, protein was extracted using solution A (50 mM tris-HCl (pH 7.5), 150 mM NaCl, 5 mM EDTA, 1% Triton X-100, 1 mM PMSF, and 1× protease inhibitor). An aliquot of the extracts was immunoblotted with the indicated antibodies. The remaining extracts were immunoprecipitated using Sepharose beads bound to anti-Hus1 or anti-NS2B antibodies at 4°C overnight. After washing the Sepharose beads four times with solution B (50 mM tris-HCl (pH 7.5), 150 mM NaCl, 0.2% Triton X-100, and 1 mM PMSF), proteins were eluted by heating the beads to 95°C in 1× SDS-polyacrylamide gel electrophoresis loading buffer (50 mM tris-HCl (pH 6.8), 2% SDS, 6% glycerol, and 2% β -mercaptoethanol). The eluate was analysed by immunoblotting with the indicated antibodies.

Immunofluorescence staining and confocal imaging

WT and *ERp57*^{-/-} RD cells were seeded in 24-well plates with a pre-coated coverslip in each well. After indicated time of infection, cells were fixed with 4% paraformaldehyde for 15 min and permeabilized in 0.2% Triton X-100 for 15 min at room temperature and blocked in PBS containing 20% bovine serum and 1% BSA. Cells would be stained with the indicated primary antibodies overnight at 4°C. Cover glasses were washed 3–5 times with PBS before incubated with immunofluorescent secondary antibodies. Samples were then washed with PBS and stained with DAPI for 10 min. DAPI dilution would be removed before cover glasses were mounted onto slides. Images were taken by Zeiss LSM 880 confocal microscope and analysed using ZEN (Carl Zeiss) and Image J software.

Statistical analysis

All data were analysed using Prism software (Graph-Pad). Statistical evaluation was performed by two-way Student's *t* test. Data are means \pm SEM, and *P* values are indicated by **P* < 0.05, ***P* < 0.01, ****P* < 0.001, **** *P* < 0.0001. All cellular experiments were repeated at least three times.

Disclosure statement

No potential conflict of interest was reported by the author (s).

Funding

The work was partially supported by grants RGC General Research Fund of Hong Kong Special Administrative Region [11104020] and Strategic funds from The City University of Hong Kong to M. He [7005874, 7020032, 9680149].

Author contributions

RW and MLH designed and supervised the study. LS and MLH supervised experiments. YW, DS, YL, LQ, QW, HH, MW, YF did experiments and collected data. YW and DS analysed the data. YW and MLH drafted the manuscript.

References

- [1] Abushouk AI, Negida A, Ahmed H. An updated review of Zika virus. *J Clin Virol.* 2016;84:53–58. doi:10.1016/j.jcv.2016.09.012
- [2] Hammack C. Zika virus infection induces DNA damage response in human neural progenitors that enhances viral replication. *J Virol.* 2019;93:e00638–19. doi:10.1128/JVI.00638-19
- [3] Atif M, Azeem M, Sarwar MR, et al. Zika virus disease: a current review of the literature. *Infection.* 2016;44:695–705. doi:10.1007/s15010-016-0935-6
- [4] Agrelli A, Moura RR, Crovella S, et al. Zika virus entry mechanisms in human cells. *Infect Genet Evol.* 2019;69:22–29. doi:10.1016/j.meegid.2019.01.018
- [5] Boeuf P, Drummer HE, Richards JS, et al. The global threat of Zika virus to pregnancy: epidemiology, clinical perspectives, mechanisms, and impact. *BMC Med.* 2016;14:1–9. doi:10.1186/s12916-016-0660-0
- [6] Faria NR. Zika virus in the Americas: early epidemiological and genetic findings. *Science.* 2016;352:345–349. doi:10.1126/science.aaf5036
- [7] Heinz FX, Stiasny K. The antigenic structure of Zika virus and its relation to other flaviviruses: implications

- for infection and immunoprophylaxis. *Microbiol Mol Biol Rev.* 2017;81:e00055-16. doi:10.1128/MMBR.00055-16
- [8] Saiz J-C. Zika virus: the latest newcomer. *Front Microbiol.* 2016;7:496.
- [9] Sager G, Gabaglio S, Sztul E, et al. Role of host cell secretory machinery in Zika virus life cycle. *Viruses.* 2018;10:559. doi:10.3390/v10100559
- [10] Muller DA, Young PR. The flavivirus NS1 protein: molecular and structural biology, immunology, role in pathogenesis and application as a diagnostic biomarker. *Antivir Res.* 2013;98:192–208. doi:10.1016/j.antiviral.2013.03.008
- [11] Liang Q, Luo Z, Zeng J, et al. Zika virus NS4A and NS4B proteins deregulate Akt-mTOR signaling in human fetal neural stem cells to inhibit neurogenesis and induce autophagy. *Cell Stem Cell.* 2016;19:663–671. doi:10.1016/j.stem.2016.07.019
- [12] Chiramel AI, Best SM. Role of autophagy in Zika virus infection and pathogenesis. *Virus Res.* 2018;254:34–40. doi:10.1016/j.virusres.2017.09.006
- [13] Lei J. Crystal structure of Zika virus NS2B-NS3 protease in complex with a boronate inhibitor. *Science.* 2016;353:503–505. doi:10.1126/science.aag2419
- [14] Melian EB. West Nile virus NS2A protein facilitates virus-induced apoptosis independently of interferon response. *J Gen Virol.* 2013;94:308. doi:10.1099/vir.0.047076-0
- [15] Shafee N, AbuBakar S. Dengue virus type 2 NS3 protease and NS2B-NS3 protease precursor induce apoptosis. *J Gen Virol.* 2003;84:2191–2195. doi:10.1099/vir.0.19022-0
- [16] Bhattacharjee R, Jolly LA, Corbett MA, et al. Compromised transcription-mRNA export factor THOC2 causes R-loop accumulation, DNA damage and adverse neurodevelopment. *Nat Commun.* 2024;15:1210. doi:10.1038/s41467-024-45121-5
- [17] Qi R, Sammler E, Gonzalez-Hunt CP, et al. A blood-based marker of mitochondrial DNA damage in Parkinson's disease. *Sci Transl Med.* 2023;15:eabo1557. doi:10.1126/scitranslmed.abo1557
- [18] Welch G, Tsai LH. Mechanisms of DNA damage-mediated neurotoxicity in neurodegenerative disease. *EMBO Rep.* 2022;23:e54217. doi:10.15252/embr.202154217
- [19] Schwab N, Tator C, Hazrati L-N. Dna damage as a marker of brain damage in individuals with history of concussions. *Lab Invest.* 2019;99:1008–1018. doi:10.1038/s41374-019-0199-8
- [20] Ciccio A, Elledge SJ. The DNA damage response: making it safe to play with knives. *Mol Cell.* 2010;40:179–204. doi:10.1016/j.molcel.2010.09.019
- [21] Matsuoka S, Ballif BA, Smogorzewska A, et al. ATR and ATR substrate analysis reveals extensive protein networks responsive to DNA damage. *Science.* 2007;316:1160–1166. doi:10.1126/science.1140321
- [22] Bedard K, Szabo E, Michalak M, et al. Cellular functions of endoplasmic reticulum chaperones calreticulin, calnexin, and ERp57. *Int Rev Cytol.* 2005;245:91–121. doi:10.1016/S0074-7696(05)45004-4
- [23] Jain S, McGinnes LW, Morrison TG. Overexpression of thiol/disulfide isomerases enhances membrane fusion directed by the Newcastle disease virus fusion protein. *J Virol.* 2008;82:12039–12048. doi:10.1128/JVI.01406-08
- [24] De Marco F. Oxidative stress in HPV-driven viral carcinogenesis: redox proteomics analysis of HPV-16 dysplastic and neoplastic tissues. *PLoS One.* 2012;7:e34366. doi:10.1371/journal.pone.0034366
- [25] Kim Y, Chang K-O. Protein disulfide isomerases as potential therapeutic targets for influenza A and B viruses. *Virus Res.* 2018;247:26–33. doi:10.1016/j.virusres.2018.01.010
- [26] Wan Q, Song D, Li H, et al. Stress proteins: the biological functions in virus infection, present and challenges for target-based antiviral drug development. *Signal Transduct Target Ther.* 2020;5:1–40. doi:10.1038/s41392-019-0089-y
- [27] Wang M. Oblongifolin M, an active compound isolated from a Chinese medical herb *Garcinia oblongifolia*, potently inhibits enterovirus 71 reproduction through downregulation of ERp57. *Oncotarget.* 2015;7:8797–8808. doi:10.18632/oncotarget.7122
- [28] Dong Q, Men R, Dan X, et al. Hsc70 regulates the IRES activity and serves as an antiviral target of enterovirus A71 infection. *Antiviral Res.* 2018;150:39–46. doi:10.1016/j.antiviral.2017.11.020
- [29] Wu M, Wan Q, Dan X, et al. Targeting Ser78 phosphorylation of Hsp27 achieves potent antiviral effects against enterovirus A71 infection. *Emerg Microbes Infect.* 2024;13:2368221. doi:10.1080/22221751.2024.2368221
- [30] Li H, Wang X, Wang Y, et al. Secreted LRPAP1 binds and triggers IFNAR1 degradation to facilitate virus evasion from cellular innate immunity. *Signal Transduct Target Ther.* 2023;8:1–13. doi:10.1038/s41392-022-01259-6
- [31] Zhou F, Wan Q, Chen Y, et al. Pim1 kinase facilitates Zika virus replication by suppressing host cells' natural immunity. *Signal Transduct Target Ther.* 2021;6:207. doi:10.1038/s41392-021-00539-x
- [32] Giraldo MI, Xia H, Aguilera-Aguirre L, et al. Envelope protein ubiquitination drives entry and pathogenesis of Zika virus. *Nature.* 2020;585:414–419. doi:10.1038/s41586-020-2457-8
- [33] Retallack H, Di Lullo E, Arias C, et al. Zika virus cell tropism in the developing human brain and inhibition by azithromycin. *Proc Nat Acad Sci.* 2016;113:14408–14413. doi:10.1073/pnas.1618029113
- [34] Dias SSG, Cunha-Fernandes T, Souza-Moreira L, et al. Metabolic reprogramming and lipid droplets are involved in Zika virus replication in neural cells. *J Neuroinflammation.* 2023;20:61. doi:10.1186/s12974-023-02736-7
- [35] Agholme L, Lindström T, Kågedal K, et al. An in vitro model for neuroscience: differentiation of SH-SY5Y cells into cells with morphological and biochemical characteristics of mature neurons. *J Alzheimers Dis JAD.* 2010;20:1069–1082. doi:10.3233/JAD-2010-091363
- [36] Muthuraj PG, Sahoo PK, Kraus M, et al. Zika virus infection induces endoplasmic reticulum stress and apoptosis in placental trophoblasts. *Cell Death Discov.* 2021;7:1–17. doi:10.1038/s41420-020-00379-8
- [37] Almeida LT, Ferraz AC, da Silva Caetano CC, et al. Zika virus induces oxidative stress and decreases antioxidant enzyme activities in vitro and in vivo. *Virus Res.* 2020;286:198084. doi:10.1016/j.virusres.2020.198084
- [38] Ledur PF, Karmirian K, Pedrosa CD, et al. Zika virus infection leads to mitochondrial failure, oxidative stress and DNA damage in human iPSC-derived astrocytes. *Sci Rep.* 2020;10:1218. doi:10.1038/s41598-020-57914-x

- [39] Ano Y. Oxidative damage to neurons caused by the induction of microglial NADPH oxidase in encephalomyocarditis virus infection. *Neurosci Lett*. 2010;469:39–43. doi:10.1016/j.neulet.2009.11.040
- [40] Hahm JY, Park J, Jang E-S, et al. 8-Oxoguanine: from oxidative damage to epigenetic and epitranscriptional modification. *Exp Mol Med*. 2022;54:1626–1642. doi:10.1038/s12276-022-00822-z
- [41] Roy IM, Nadar PS, Khurana S. Neutral comet assay to detect and quantitate DNA double-strand breaks in hematopoietic stem cells. *Bio-Protoc*. 2021;11:e4130.
- [42] Bakkenist CJ, Kastan MB. Dna damage activates ATM through intermolecular autophosphorylation and dimer dissociation. *Nature*. 2003;421:499–506. doi:10.1038/nature01368
- [43] Burma S, Chen BP, Murphy M, et al. Atm phosphorylates histone H2AX in response to DNA double-strand breaks. *J Biol Chem*. 2001;276:42462–42467. doi:10.1074/jbc.C100466200
- [44] Hirai I, Sasaki T, Wang H-G. Human hRad1 but not hRad9 protects hHus1 from ubiquitin–proteasomal degradation. *Oncogene*. 2004;23:5124–5130. doi:10.1038/sj.onc.1207658
- [45] Ghouzi VE, Bianchi FT, Molineris I, et al. Zika virus elicits P53 activation and genotoxic stress in human neural progenitors similar to mutations involved in severe forms of genetic microcephaly and p53. *Cell Death Dis*. 2016;7:e2440–e2440. doi:10.1038/cddis.2016.266
- [46] Ji W, Luo G. Zika virus NS5 nuclear accumulation is protective of protein degradation and is required for viral RNA replication. *Virology*. 2020;541:124–135. doi:10.1016/j.virol.2019.10.010
- [47] Ci Y, Liu ZY, Zhang NN, et al. Zika NS1–induced ER remodeling is essential for viral replication. *J Cell Biol*. 2019;219:e201903062. doi:10.1083/jcb.201903062
- [48] Phoo WW, Li Y, Zhang Z, et al. Structure of the NS2B–NS3 protease from Zika virus after self-cleavage. *Nat Commun*. 2016;7:13410. doi:10.1038/ncomms13410
- [49] Li H, Saucedo-Cuevas L, Yuan L, et al. Zika virus protease cleavage of host protein septin-2 mediates mitotic defects in neural progenitors. *Neuron*. 2019;101:1089–1098.e4. doi:10.1016/j.neuron.2019.01.010
- [50] Kaplan A, Gaschler MM, Dunn DE, et al. Small molecule-induced oxidation of protein disulfide isomerase is neuroprotective. *Proc Natl Acad Sci*. 2015;112:E2245–E2252. doi:10.1073/pnas.1500439112
- [51] Chamberlain N, Ruban M, Mark ZF, et al. Protein disulfide isomerase A3 regulates influenza neuraminidase activity and influenza burden in the lung. *Int J Mol Sci*. 2022;23:1078. doi:10.3390/ijms23031078
- [52] Zhou X, Li G, Kaplan A, et al. Small molecule modulator of protein disulfide isomerase attenuates mutant huntingtin toxicity and inhibits endoplasmic reticulum stress in a mouse model of Huntington’s disease. *Hum Mol Genet*. 2018;27:1545–1555. doi:10.1093/hmg/ddy061
- [53] Khongwichit S, Sornjai W, Jitobaom K, et al. A functional interaction between GRP78 and Zika virus E protein. *Sci Rep*. 2021;11:393. doi:10.1038/s41598-020-79803-z
- [54] Gonzalez-Perez P, Woehlbier U, Chian RJ, et al. Identification of rare protein disulfide isomerase gene variants in amyotrophic lateral sclerosis patients. *Gene*. 2015;566:158–165. doi:10.1016/j.gene.2015.04.035
- [55] Cao SS, Kaufman RJ. Endoplasmic reticulum stress and oxidative stress in cell fate decision and human disease. *Antioxid Redox Signal*. 2014;21:396–413.
- [56] Gladwyn-Ng I, Córdón-Barris L, Alfano C, et al. Stress-induced unfolded protein response contributes to Zika virus-associated microcephaly. *Nat Neurosci*. 2018;21:63–71. doi:10.1038/s41593-017-0038-4
- [57] El-Amine R, Germini D, Zakharova VV, et al. HIV-1 Tat protein induces DNA damage in human peripheral blood B-lymphocytes via mitochondrial ROS production. *Redox Biol*. 2018;15:97–108. doi:10.1016/j.redox.2017.11.024
- [58] Li P, Wu J, Liu S, et al. The RNA polymerase of cytoplasmically replicating Zika virus binds with chromatin DNA in nuclei and regulates host gene transcription. *Proc Natl Acad Sci*. 2022;119:e2205013119. doi:10.1073/pnas.2205013119
- [59] Sornjai W, Promma P, Prierkiew S, et al. The interaction of GRP78 and Zika virus E and NS1 proteins occurs in a chaperone-client manner. *Sci Rep*. 2024;14:1–18. doi:10.1038/s41598-024-61195-z
- [60] Coluccia A, Puxeddu M, Nalli M, et al. Discovery of Zika virus NS2B/NS3 inhibitors that prevent mice from life-threatening infection and brain damage. *ACS Med Chem Lett*. 2020;11:1869–1874. doi:10.1021/acsmchemlett.9b00405
- [61] Lee H, Ren J, Nocadello S, et al. Identification of novel small molecule inhibitors against NS2B/NS3 serine protease from Zika virus. *Antiviral Res*. 2017;139:49–58. doi:10.1016/j.antiviral.2016.12.016
- [62] Falgout B, Pethel M, Zhang YM, et al. Both nonstructural proteins NS2B and NS3 are required for the proteolytic processing of dengue virus nonstructural proteins. *J Virol*. 1991;65(5):2467–2475. doi:10.1128/jvi.65.5.2467-2475.1991
- [63] Kumar A, Kumar P, Mishra PM, et al. Investigating the folding dynamics of NS2B protein of Zika virus. *Virology*. 2023;584:24–36. doi:10.1016/j.virol.2023.04.012
- [64] Xing H. Zika NS2B is a crucial factor recruiting NS3 to the ER and activating its protease activity. *Virus Res*. 2020;275:197793. doi:10.1016/j.virusres.2019.197793
- [65] Li C, Huang L, Sun W, et al. Saikosaponin D suppresses enterovirus A71 infection by inhibiting autophagy. *Signal Transduct Target Ther*. 2019;4:1–12. doi:10.1038/s41392-018-0034-5